The bile acid TUDCA improves glucose metabolism in streptozotocin-induced Alzheimer's disease mice model

Lucas Zangerolamo[1], Jean F. Vettorazzi[2], Carina Solon[3], Gabriela A. Bronczek[1], Daiane F. Engel[3], Mirian A. Kurauti[4], Gabriela M. Soares[1], Karina S. Rodrigues[1], Lício A. Velloso[3], Antonio C. Boschero[1], Everardo M. Carneiro[1], Helena C. L. Barbosa[1*]

[1] Obesity and Comorbidities Research Center, Department of Structural and Functional Biology, University of Campinas, UNICAMP, Campinas, Sao Paulo, Brazil.

[2] Educational Union of Cascavel, UNIVEL, Cascavel, Parana, Brazil.

[3] Laboratory of Cell Signaling, Obesity and Comorbidities Research Center, University of Campinas, UNICAMP, Campinas, Sao Paulo, Brazil.

[4] Department of Physiological Sciences, State University of Maringa, UEM, Maringa, Parana, Brazil.

***Correspondence:** Helena Cristina L. Barbosa, Obesity and Comorbidities Research Center, University of Campinas, UNICAMP, Campinas, Sao Paulo, CEP: 13083-864, Brazil.

Tel.: +55 19 3521 0011. Fax: +55 19 3521 6185.

E-mail address: bsampaio@unicamp.br

ABSTRACT

Alzheimer's disease (AD) is a neurodegenerative disorder and the major cause of dementia. According to predictions of the World Health Organization, more than 150 million people worldwide will suffer from dementia by 2050. An increasing number of studies have associated AD with type 2 diabetes mellitus (T2DM), since most of the features found in T2DM are also observed in AD, such as insulin resistance and glucose intolerance. In this sense, some bile acids have emerged as new therapeutic targets to treat AD and metabolic disorders. The taurine conjugated bile acid, tauroursodeoxycholic (TUDCA), reduces amyloid oligomer accumulation and improves cognition in APP/PS1 mice model of AD, and also improves glucose-insulin homeostasis in obese and type 2 diabetic mice. Herein, we investigated the effect of TUDCA upon glucose metabolism in streptozotocin-induced AD mice model (Stz). The Stz mice that received 300 mg/kg TUDCA during 10 days (Stz+TUDCA), showed improvement in glucose tolerance and insulin sensitivity, reduced fasted and fed glycemia, increased islet mass and β-cell area, as well as increased glucose-stimulated insulin secretion, compared with Stz mice that received only PBS. Stz+TUDCA mice also displayed lower neuroinflammation, reduced protein content of amyloid oligomer in the hippocampus, improved memory test and increased protein content of insulin receptor β-subunit in the hippocampus. In conclusion, TUDCA treatment enhanced glucose homeostasis in the streptozotocin-induced Alzheimer's disease mice model, pointing this bile acid as a good strategy to counteract glucose homeostasis disturbance in AD pathology.

Keywords: TUDCA, Alzheimer's disease, insulin resistance; glucose homeostasis; neuroinflammation.

1 INTRODUCTION

Alzheimer's disease (AD), a neurodegenerative disorder, is the major form of dementia in elderly people (Wang, Gu, Masters, & Wang, 2017). AD pathogenesis is characterized by accumulation and deposits of extracellular amyloid-beta protein (Aβ) (Selkoe, 2001), intracellular neurofibrillary tangles (NFTs) containing hyperphosphorylated TAU protein (Rudrabhatla, Jaffe, & Pant, 2011) and neuroinflammation (Heneka et al., 2015), mainly in the frontal cortex and hippocampus, regions highly involved in memory, resulting in neuronal death, progressively memory deficits and cognitive disabilities (Walsh & Selkoe, 2004).

Accumulating evidences have been shown that insulin resistance may be one of the major risk factors associated with AD (Bedse, Di Domenico, Serviddio, & Cassano, 2015), providing a link between type 2 diabetes mellitus (T2DM) and AD. In T2DM, insulin resistance results in deposition of Aβ plaques, mitochondrial dysfunction and inflammation in peripheral tissues (Beeler, Riederer, Waeber, & Abderrahmani, 2009; Esser, Legrand-Poels, Piette, Scheen, & Paquot, 2014; Lowell & Shulman, 2005). These features are also found in AD patients (Mittal & Katare, 2016), suggesting that type 2 diabetic patients have increased risk of developing AD (Clarke et al., 2015; Vandal et al., 2015).

T2DM induction in mouse models of AD, increases Aβ accumulation, TAU phosphorylation, vascular complications and cognitive impairment (Vandal et al., 2015). In addition, impaired glucose tolerance and insulin resistance are also found in mouse models of AD (Clarke et al., 2015; Macklin et al., 2017; Shinohara & Sato, 2017). Besides that, reduced glucose utilization and deficient energy metabolism have also been observed in AD pathogenesis (Yin, Sancheti, Patil, & Cadenas, 2016).

Streptozotocin (STZ) is a chemical commonly used in the treatment of metastasizing pancreatic islet cell tumors (Eleazu, Eleazu, Chukwuma, & Essien, 2013) and to induce type 1 and type 2 diabetes mellitus in rodents (Furman, 2015; Nath, Ghosh, & Choudhury, 2017). On the other hand, sub-diabetogenic doses of STZ administration by intracerebroventricular (ICV) injections induces: a) Aβ accumulation (Salkovic-Petrisic, Osmanovic, Grünblatt, Riederer, & Hoyer, 2009), b) activation of microglial cells and neuroinflammation (Kamat et al., 2016; Rai, Kamat, Nath, & Shukla, 2014), c) brain insulin resistance, d) glucose and energy metabolism disturbances (Müller, Nitsch, Wurtman, & Hoyer, 1998), e) cholinergic deficiency, and f) oxidative stress (Salkovic-Petrisic et al., 2009), mainly in the hippocampus and cerebral cortex, resulting in cognitive dysfunction (Plaschke & Hoyer, 1993). Therefore, this model is widely used and accepted, once it features behavioral, neurochemical and structural alterations that mimics human sporadic AD (SAD) (Salkovic-Petrisic & Hoyer, 2007), making of it a very useful one for investigating the effects of chemical compounds that might attenuate and treat SAD.

In this context, the bile acids, especially the tauroursodeoxycholic acid (TUDCA), has shown a great therapeutic potential for the prevention and treatment of AD in mice. TUDCA is an endogenous bile acid, produced from the conjugation of the ursodeoxycholic acid (UDCA) with the amino acid taurine, and is able to cross the blood-brain barrier (Keene et al., 2001; Lo, Callaerts-Vegh, Nunes, Rodrigues, & D'Hooge, 2013). In APP/PS1 mice model, an important one for AD, it has been demonstrated that TUDCA prevents Aβ plaques accumulation, reduces synaptic loss and rescues cognitive deficits, by: a) modulating γ-secretase activity and processing of amyloid precursor protein (APP), b) abrogating glycogen synthase kinase 3 beta (GSK3β) hyperactivity and averting TAU hyperphosphorylation, and c) decreasing

activation of astrocytes and microglia (Dionísio et al., 2015; Nunes et al., 2012). TUDCA supplementation in food also prevents the spatial, recognition and contextual memory defects observed in APP/PS1 mice (Lo et al., 2013). Moreover, TUDCA improves glucose tolerance, insulin sensitivity and insulin clearance in obese mice (Vettorazzi et al., 2017), and increases glucose-induced insulin secretion in isolated pancreatic islets from mice (Vettorazzi et al., 2016). However, the effect of TUDCA upon glucose metabolism in an experimental AD mice model remains unclear. Therefore, we aimed to evaluate the possible effects of TUDCA attenuating the impairment in glucose-insulin homeostasis in streptozotocin-induced AD mice model.

2 MATERIAL AND METHODS

2.1 Animals

Two-month-old male C57BL/6 mice from the University of Campinas facilities were used throughout this study. Mice were housed in a quiet, temperature-and-humidity-controlled room with 12-hr light/12-hr dark cycle and *ad libitum* access to food and water during the entire experiment. All procedures were approved by the Animal Care Committee at the University of Campinas (license numbers: 4698-1/2017 and 5022-1/2018), and were conducted in accordance to the last revision of the National Institutes of Health (NIH) guide for the care and use of laboratory animals.

2.2 Intracerebroventricular (ICV) Injections and TUDCA treatment

Mice were previously anesthetized with a mix of ketamine and xylazin. After that, mice were restrained onto a stereotaxic apparatus (Stoelting Apparatus) and STZ (3 mg/kg, ICV) was injected bilaterally into the lateral ventricles to produce the ICV-STZ AD mice model. The control mice (Ctl) were submitted to the same procedure, but with

vehicle (citrate buffer 0.05 mol/L, pH 4.5) injection. STZ was diluted in citrate buffer immediately before injection. The injection of STZ was performed using a Hamilton syringe (model 705) and the coordinates used from the bregma were: AP −0.5 mm; ML ±1.1 mm; DV −2.8 mm, based on the previously published method (Ravelli, Rosário, Camarini, Hernandes, & Britto, 2017). A total of 1.5 μL of STZ or citrate buffer was infused in each lateral ventricle and it was conducted at a rate of 0.5 μL/min. After 2 days, the injection of STZ or citrate buffer was repeated (1.5 mg/kg per day of injection). To confirm whether STZ was administered exactly into the cerebral ventricles, brains were dissected and macroscopically examined immediately after the procedure.

ICV-STZ mice were randomly selected and divided into 2 groups: Stz+TUDCA group, that received 300 mg/kg of TUDCA (Calbiochem, São Paulo, Brazil; cat. 580549) intraperitoneally (i.p.) and the Stz group, that received only the vehicle phosphate buffered saline (PBS). The injections of TUDCA or PBS were administered during 10 days, beginning 6 days after the first application of STZ. Stz+TUDCA and Stz mice were compared to Ctl mice, which received PBS injections during the experimental procedures.

2.3 Intraperitoneal glucose and insulin tolerance tests (ipGTT and ipITT)

At the end of TUDCA treatment, mice were subjected to ipGTT and ipITT. To perform the ipGTT, overnight fasted (12 hr) mice received, intraperitoneally, a dose of glucose by the order of 2 g/kg of body weight. The blood samples were taken from the tail vein before the procedure (time 0); and 15, 30, 60, 90 and 120 min after the glucose load. The area under the curve (AUC) of blood glucose during the ipGTT was then

calculated. To perform ipITT, mice were maintained fasted for 4 hr and glycemia was measured before (time 0), and 3, 6, 9, 12, 15 and 18 min after the intraperitoneal administration of 0.75 U/kg insulin. The kITT (constant rate for glucose disappearance) was calculated as previously described (Akinmokun, Selby, Ramaiya, & Alberti, 1992). In both tests, blood glucose was measured using glucose strips on an Accu-Check Performa II glucometer (Roche, Sao Paulo, BRA).

2.4 Plasmatic Insulin and C-Peptide Measurements

To evaluate the levels of plasma insulin and c-peptide, at the end of TUDCA treatment mice were subjected to 16-hr fasting, and blood samples were then taken from the tail vein before (time 0), and 30 and 60 min after a glucose gavage (2 g/kg body weight). Blood samples were drawn in heparin capillary tubes, centrifuged at 11.000 rpm, 4ºC for 15 min, to obtain the plasma. Plasma insulin and c-peptide were measured using specific commercial enzyme-linked immunosorbent assay (ELISA) kits (Chrystal Chem, Inc, Downers Grove, IL, USA; cat No. #90080 and #90050); following the manufacturer's instructions. The c-peptide:insulin ratio was calculated for each time point to determine the insulin clearance, as previously described (Kurauti et al., 2016).

2.5 Novel Object Recognition Test

The novel object recognition test (NORT) is used to evaluate cognition, and is based on the spontaneous tendency of rodents to spend more time exploring novel objects than a familiar one in an open field arena. This behavioral task consisted of three phases: habituation, familiarization and test phase. In the habituation phase (first day), mice were habituated to the open field arena (20 cm high x 32 cm wide x 33 cm long) in the absence of objects, during 10 min. On the second day (familiarization phase), each

mouse was placed in the middle of the arena, containing two identical objects (A and B), arranged in a symmetric position from de center of the arena, for 10 min. To avoid coercion to explore the objects, mice were released with their back to the objects. On the third day (test phase), one of the familiar objects (B) was replaced for a new object (C) and mice returned to the open field arena and were allowed to explore both objects for 10 min. The arena and the objects were cleaned with 10% ethanol between each mouse exposure. Object exploration was defined as mice sniffing, licking, or touching the object with their nose or with the forepaws or directing the nose to the object at a distance of ≤ 1 cm. The total exploration time of the objects during the 10 min was quantified in the familiarization and test phases. The preference index (PI) for the novel object was calculated as a percentage of the time spent exploring the new object (C) over the total time spent exploring both objects (B+C) during the test phase; PI (%) = (C/B+C) x 100. Therefore, a preference index above 50% indicates novel object preference, below 50% familiar object preference, and 50% no preference (Antunes & Biala, 2012).

2.6 Body parameters and tissue collection

The body weight of all mice was evaluated weekly throughout the experimental procedure. For the determination of fasting glycemia, the mice were fasted for 12 hr, and then the measurement of blood glucose was made by Accu-Check Performa II glucometer (Roche, São Paulo, BR). Blood glucose was measured again 3 hr postprandial (fed state). At the end of TUDCA treatment, mice (4 hr fasting) were anesthetized with isoflurane and killed by decapitation. Brain was weighted, and the hippocampus, pancreas and liver were collected for posterior analyses. In addition, the

perigonadal and retroperitoneal fat pads, as well as gastrocnemius muscle were dissected and weighed.

2.7 Glucose-stimulated insulin secretion in pancreatic islets

The pancreatic islets of the mice were isolated by the collagenase method (Boschero et al., 1995). Five islets from each mouse were preincubated for 1 hr in Krebs–Henseleit buffer solution (KHBS) containing 0.5 g/L bovine serum albumin and 5.6 mM glucose (pH 7.4, with 95% O_2 and 5% CO_2 at 37°C). Subsequently, the islets were incubated for an additional hour in KHBS containing 2.8 or 11.1 mM glucose. The supernatant was collected to evaluate the insulin secretion, and the remaining islets were homogenized in an alcohol–acid solution to measure total insulin content. Insulin secretion and total insulin content were measured by ELISA kit (Mercodia AB; cat No. 10-1247-01), according to the companies' instructions.

2.8 RNA extraction and quantitative real-time PCR analysis

Liver and hippocampus samples were submitted to RNA extraction using 1 mL TRIzol® Reagent (Invitrogen™, Thermo Fisher Scientific Inc, Waltham, MA, USA; cat. 15596026), and the mRNA was extracted following the manufacturer's instructions. To prepare the cDNA, 1 μg of total mRNA and High-Capacity cDNA Reverse Transcription Kit (Applied Biosystems™, Thermo Fisher Scientific Inc, Waltham, MA, USA) were used. Real time PCR was performed on 7500 Fast Real-time PCR System (Applied Biosystems™) using Fast SYBR® Green Master Mix (Applied Biosystems™). Glyceraldehyde-3-phosphate dehydrogenase (GAPDH) was used as endogenous control. The primers sequences, showed in Table 1, were designed and purchased from IDT®- Integrated DNA Technologies.

2.9 Western blot analysis

Hippocampus and liver samples were homogenized with 500 µL of lysis buffer (10 mM EDTA, 100 mM tris base, 100 mM sodium pyrophosphate, 100 mM sodium fluoride, 10 mM sodium orthovanadate, 2 mM phenylmethylsulfonyl fluoride, 1% triton X-100 and 1 µg/mL aprotinin). Protein concentration was measured using Bradford reagent (BioAgency Biotecnologia, São Paulo, Brazil). Protein samples 30 µg were homogenized and boiled (5 min at 100 °C) in a Laemmli buffer, after that, proteins were separated by electrophoresis in a 10% polyacrylamide gel. The transfer to nitrocellulose membranes was performed in a Trans Blot transfer for 2 hr in 90 V, with tris/glycine buffer. The membranes were blocked in a tris-buffered saline (10 mM tris base, 150 mM NaCl and 0.25% (vol./vol.) of tween 20) containing 5% (wt./vol.) bovine serum albumin (BSA), for 1 hr at room temperature. After, the membranes were incubated overnight at 4°C with primary antibodies against Amyloid Oligomer (Millipore cat. ab9234), IDE (abcam cat. ab32216), CEACAM-1 (Cell Signaling cat. 14771), IR β-subunit (Cell Signaling cat. 3025), p-AKT (Ser473) (Cell Signaling cat. 9271) and AKT (Cell Signaling cat. 9272). GAPDH (Sigma Aldrich, cat. G9545) was used as an internal control of the experiment. Visualization of specific protein bands was performed by incubating the membranes with appropriate secondary antibodies and bands detection was performed by chemiluminescence in the Amersham Imager 600 (GE Healthcare Life Sciences, Buckinghamshire, UK). The band intensities were quantified by optical densitometry using ImageJ software (National Institutes of Health, Maryland, USA).

AKT phosphorylation was assessed as previously described (Zangerolamo et al., 2019) with minor modifications. Briefly, the mice were anesthetized and fragments of the liver, perigonadal adipose tissue and skeletal muscle (gastrocnemius) were collected.

Subsequently, 4 U/kg insulin was administered into the cava vein, and liver, perigonadal adipose tissue and gastrocnemius samples were again collected after 5 min. The tissues were processed and evaluated as described above.

2.10 Immunofluorescence staining and quantification

Mice were deeply anesthetized (ketamine 80 mg/Kg and xylazine 10 mg/Kg i.p.) and were perfused through the left cardiac ventricle with 0.9% saline solution, followed by 4% paraformaldehyde in 0.1 M PBS, pH 7.4. After perfusion, the brains were removed, post-fixed in the same fixative solution for 24 hr at room temperature and cryoprotected by immersion in a 30%, then 40% sucrose solution in PBS at 4°C. OCT frozen brains were then submitted to coronal sectioning (20 μm thickness) using the cryostat (LEICA Microsystems®, CM1860, Buffalo Grove, IL, USA). Sections were first blocked using 10% goat serum (GS) diluted in PBS containing 2% triton X-100 (PBS-Tx) for 2 hr at room temperature. Sections were incubated overnight at 4°C in rabbit anti-Iba-1 primary antibody (1:200; Wako LKN4881). After washing in PBS, tissue sections were incubated with anti-rabbit FITC (1:200; Santa Cruz sc2012) in 3% GS diluted in 0.5% PBS-Tx for 2h at room temperature. Thereafter, the sections were washed in PBS and then incubated with 0.5 g/mL DAPI (Invitrogen, D1306) for 10 min, washed, mounted in Vectashield (Vector, H-1200) and covered with coverslips. Finally, images from mouse hippocampus were obtained with a confocal microscope (Upright LSM780-NLO Zeiss) and fluorescence intensity was quantified with ImageJ software (National Institutes of Health, Maryland, USA).

2.11 Pancreas Morphometry and Immunohistochemistry

Pancreas samples were collected from four animals from each group and fixed in 10% formalin, embedded in Paraplast (Sigma Aldrich, St Louis, MO, USA), sectioned into slices of 5 µm and adhered to individual silanized glasses. The first and the 50th sections were immunoperoxidase-stained for insulin in order to quantify the distribution of pancreatic β-cells. Next, Paraplast was removed and the sections were rehydrated, washed with 0.5 M tris-buffered saline (TBS, pH 7.4) and treated with 0.1 M sodium citrate buffer (pH 6.0) at 100ºC for antigen retrieval. Then, the sections were washed again with TBS and blocked against endogenous peroxidase activity with 3% H_2O_2. Sections were washed with TBS and then incubated for 1 hr with TBS containing 3% BSA followed by primary antibody incubation overnight at 4ºC. The antibody used was polyclonal guinea pig anti-insulin (Dako North America, Carpinteria, CA, USA, ref. A0564) diluted at 1:100 in TBS with 3% BSA. Furthermore, there was an incubation in the presence of a secondary antibody for 1 hr. The antibody used was anti-guinea pig IgG, diluted at 1:200. Cells that were positive for insulin were detected with diaminobenzidine (DAB) solution (0.1% DAB and 0.02% H_2O_2 in TBS). Lastly, the sections were rapidly stained with Harris' hematoxylin and mounted for microscopic observation. All the islets present in the sections were covered systematically by capturing images with a digital camera coupled to a microscope (Olympus DP71; Olympus BX60, Japan). Pancreatic islets and β-cells areas were measured using ImageJ software (National Institutes of Health, Bethesda, MD, USA).

2.12 Statistical analysis

The data were presented as means ± standard errors media (SEM), analyzed by one-way analysis of variance (ANOVA) followed by the Tukey post-hoc-test ($P \leq 0.05$), using GraphPad Prism version 6.00 software (GraphPad Inc., CA, USA).

3 RESULTS

3.1 TUDCA treatment normalizes pathological neuromarkers in STZ-induced AD mice

To characterize our AD mice model, the brain of the mice was weighed and the protein content of amyloid oligomer, as well as the fluorescence of the microglia activator Iba-1, were measured in the hippocampus. In addition, we performed a behavioral test, the NORT, to evaluate cognition. As expected, Stz mice presented reduced brain weight (Figure 1A), increased levels of amyloid oligomer (Figure 1B) and increased fluorescence intensity of Iba-1 (Figure 1 C-D) in the hippocampus, and besides, these mice showed no preference for the new object during the NORT (Figure 1E). In the hippocampus, we also quantified the gene expression of proinflammatory cytokines and markers of activated astrocytes, amyloidogenic and non-amyloidogenic processing of APP and neurogenesis. Also, the protein content of IR β-subunit in the hippocampus was measured. As observed in Figure 1F, Stz mice displayed an increase in mRNA levels of proinflammatory cytokines and activated astrocytes marker GFAP, compared with Ctl. Increased mRNA levels of APP and BACE-1, which is involved in amyloidogenic processing of APP, was also observed in Stz, compared with Ctl mice. Consistent with these findings, mRNA levels of the non-amyloidogenic processing of APP markers ADAM-10 and X11-α were significantly reduced in Stz mice, as well as the mRNA levels of the neurogenesis marker BDNF and the protein content of IR β-subunit (Figure 1G), which is crucial for the insulin signaling pathway. After 10-days of TUDCA treatment, our data showed that all these parameters were normalized, presenting statistically similar values compared with Ctl mice (Figure 1).

3.2 TUDCA treatment improves glucose metabolism in STZ-induced AD mice

As observed in Table 2, Stz mice showed increased body weight at the time of euthanasia, as well as increased perigonadal and retroperitoneal fat pads, compared with Ctl, whereas TUDCA treatment normalized these alterations. No differences were observed in skeletal muscle pad between the groups (Table 2).

To access glucose-insulin homeostasis, we performed ipGTT and ipITT. As expected, Stz mice presented an impairment in glucose tolerance (Figure 2A), as determined by the higher AUC of blood glucose during ipGTT, compared with Ctl mice (Figure 2B). Insulin resistance, determined by the lower kITT, was also observed in the Stz mice during the ipITT (Figure 2C-D). Regarding the fasting and fed glycemia, the Stz mice also displayed higher blood glucose values comparing with Ctl mice (Figure 2E-F). After 10-days of TUDCA treatment, we observed an improvement in glucose tolerance (Figure 2A-B), insulin sensitivity (Figure 2C-D), and, in both cases, fasting and fed glycemia (Figure 2E-F). We also quantified the protein content of AKT-phosphorylation at Ser473 before and after insulin load in the liver, adipose tissue and skeletal muscle. Stz mice presented a reduction in pAKT levels in these tissues, effect that was improved by TUDCA treatment (Supplementary Figure 1A-C).

3.3 TUDCA treatment increases glucose-stimulated insulin secretion and does not alter insulin clearance in STZ-induced AD mice

Increased plasma insulin and c-peptide levels were observed in Stz+TUDCA, compared with Stz mice, 30 min after a glucose load (Figures 3A-B). Considering that insulin clearance plays a crucial role in the regulation of plasma insulin, we evaluated

this phenomenon in these mice. It is known that pancreatic β-cells co-secrete insulin and c-peptide (1:1 ratio); however, the half-life of c-peptide is longer than that of insulin. Thus, changes in this ratio indicate an alteration in the insulin clearance. However, no differences on insulin clearance (c-peptide:insulin ratio) were observed between the groups (Figure 3C-D). In addition, we evaluated the protein content of IDE and CEACAM-1 in the liver, proteins involved in hepatic insulin clearance and, in accordance with our data, no differences in these proteins content were observed between the groups (Figure 3E-F). Finally, to explain the higher insulinemia in the Stz+TUDCA mice, we evaluated the glucose-stimulated insulin secretion in isolated pancreatic islets. After 1 hr incubation at low glucose (2.8 mM), insulin secretion was similar in both groups; however, at high glucose concentration (11.1 mM), secretion was higher in the islets from Stz+TUDCA mice, compared with the Stz mice (Figure 3G). No differences in total insulin content were observed between the groups (Figure 3H).

3.4 TUDCA treatment increases β-cell number per islet and total β-cell area in STZ-induced AD mice

We also investigated the effect of TUDCA treatment on β-cell mass and islet morphology. We observed that pancreas weight (Figure 4A), total islet area (Figure 4B), islet/pancreas section ratio (Figure 4C) and β-cell mass (Figure 4E) remained similar in both groups, Stz and Stz+TUDCA. However, islet mass (Figure 4D), β-cell number per islet (Figure 4F) and total β-cell area (Figure 4G) increased by 52%, 9% and 32%, respectively, in the Stz+TUDCA mice compared with the Stz mice. Representative figures of the histological pancreatic sections, stained for insulin, are shown in Figure 4H.

4 DISCUSSION

A crescent number of studies has shown a connection between AD and T2DM (Li, Song, & Leng, 2015). According to the Mayo Clinic Alzheimer Disease Patient Registry, 80% of AD patients present glucose tolerance impairment or have diabetes (Janson et al., 2004; Kang, Lee, & Lee, 2017). Type 2 diabetic patients are more likely to be diagnosed with dementia by 1.5 to 2-fold (Biessels, Strachan, Visseren, Kappelle, & Whitmer, 2014). Besides that, some studies have shown excess cognitive impairment and lower cognitive performance in subjects with diabetes, impaired glucose tolerance, and insulin resistance (Arvanitakis, Bennett, Wilson, & Barnes, 2010; Bruce et al., 2003; Convit, Wolf, Tarshish, & de Leon, 2003; Vanhanen et al., 1998). However, why type 2 diabetic patients display high probability of developing AD is not entirely clear.

Thus, there is a search for molecules that could improve glucose-insulin homeostasis in AD patients and mitigate the deleterious effects of this illness. In this context, the bile acid TUDCA has emerged as an important candidate due to its known benefits in glucose-insulin metabolism, improving the insulin secretion, clearance and sensitivity (Ozcan et al., 2006; Vettorazzi et al., 2017; Vettorazzi et al., 2016).

To assess the role of the bile acid TUDCA on glucose metabolism, we used the streptozotocin-induced Alzheimer's disease mice model. Our findings showed that TUDCA treatment reduced body weight and adiposity, ameliorated glucose tolerance and insulin sensitivity, improved fasted and fed glycemia, increased islet mass and β-cell area, as well as increased glucose-stimulated insulin secretion in our STZ-induced AD mice model. These mice also displayed lower neuroinflammation, reduced protein content of amyloid oligomer and higher levels of BDNF mRNA in the hippocampus, memory test improvement and increased protein content of IR β-subunit in the

hippocampus. Our study is the first one to show the therapeutic effects of TUDCA upon glucose metabolism in AD pathology, suggesting a novel approach in AD therapy.

Brain inflammation play a fundamental role during the AD progression (Kinney et al., 2018). To evaluate hippocampal inflammation in our model, we quantified the fluorescence intensity of Iba-1, a common marker of microglia activation (Franco-Bocanegra et al., 2019) and the hippocampal gene expression of proinflammatory cytokines. We observed in Stz mice an increase in the fluorescence of Iba-1 and in the gene expression of TNF-α, IL-1β, IL-6 and IFN-γ. All of these inflammatory markers were attenuated after TUDCA treatment. Whereas astrocytes also participate in the secretion of inflammatory cytokines, we assessed GFAP gene expression in the hippocampus, once it is one of the best known marker of reactive astrocytes and reactive gliosis (Pekny & Nilsson, 2005). After TUDCA treatment, we observed an attenuation of this marker, corroborating other studies that have already shown the effectiveness of TUDCA treatment in ameliorating astrocytosis and microgliosis in APP/PS1 mice (Dionísio et al., 2015; Nunes et al., 2012).

It is known that TNF-α stimulate the expression of APP and BACE-1 in primary cultures of mouse astrocytes, as well as stimulate γ-secretase activity in HEK cells, which results in the release of large amounts of Aβ peptides (Decourt, Lahiri, & Sabbagh, 2017). The attenuation of the inflammation observed in mice treated with TUDCA, contributes, at least in part, to the reduction of amyloid oligomers and cognition improvement.

Aβ is generated from transmembrane protein APP that can be processed by two pathways. First, in the amyloidogenic pathway, APP is cleaved by β-secretase and then by γ-secretase complex, resulting in Aβ production. In the non-amyloidogenic pathway,

α-secretase cleaves in the middle of the Aβ region to release the soluble APPα-fragment (Pająk, Kania, & Orzechowski, 2016; Zhang, Thompson, Zhang, & Xu, 2011). The actions of TUDCA in Aβ processing has been previously shown in APP/PS1 mice (Dionísio et al., 2015; Nunes et al., 2012) and it was observed decreased APP β and γ-secretase cleavage products, culminating in reduced Aβ1–40 and Aβ1–42 levels and amyloid plaque burden in hippocampus and frontal cortex. Here, we observed reduced mRNA levels of APP and BACE-1 after TUDCA treatment, suggesting diminished amyloidogenic cleavage of APP (Das & Yan, 2017). In addition, we also observed increased mRNA levels of X11-α, that encodes an adapter protein that binds to APP and reduces its amyloidogenic cleavage (Vandal et al., 2014), and ADAM-10, the main α-secretase that cleaves APP in the non-amyloidogenic pathway, inhibiting the formation of Aβ peptide (Peron, Vatanabe, Manzine, Camins, & Cominetti, 2018). Taken together, these data corroborate previously findings, and confirms the effect of TUDCA in modulating overall APP processing in a different animal model of AD.

Glucose intolerance and insulin resistance have also been found in AD pathology (Thambisetty et al., 2013), suggesting that impairment in peripheral metabolism can contribute to central damages. After TUDCA treatment, Stz mice presented an improvement in both glucose tolerance and insulin sensitivity, accompanied by improvement of fasting and fed glycemia. Furthermore, TUDCA treatment increased AKT phosphorylation levels in liver, perigonadal adipose tissue and skeletal muscle. Whereas AKT phosphorylation activates the translocation of GLUT4 glucose transporter to the plasma membrane of fat and muscle cells (Jiang et al., 2003), promoting glucose uptake (Abel et al., 2001; Zisman et al., 2000), the improvement in insulin sensitivity in these tissues, observed after TUDCA treatment, should contribute with the blood glucose lowering.

We also observed increased plasma c-peptide and insulin levels 30 minutes after an oral glucose administration in Stz+TUDCA mice. To assess whether the increase in plasma insulin levels was a result of increased insulin secretion or reduced insulin clearance, first, we calculated the c-peptide:insulin ratio. Besides that, we also quantified the protein content of IDE and CEACAM-1 in the liver. No difference was observed in any of these parameters, suggesting that TUDCA does not modulate insulin clearance in Stz mice. After, we evaluated glucose-stimulated insulin secretion, which was increased in Stz+TUDCA mice at high glucose concentration. Indeed, the higher insulin levels in these mice may be a direct effect of TUDCA on pancreatic β-cells.

Considering the role of TUDCA in improving pancreatic islet homeostasis, we evaluated the histology of pancreas from Stz mice, and it was observed increased β-cell number per islet and total β-cell area, as well as increased islet mass in Stz+TUDCA mice, comparing to Stz group. Taking into account the chaperone function of TUDCA in pancreatic islets and β-cells (Cadavez et al., 2014; Lee et al., 2010), the molecular mechanism whereby TUDCA improves pancreatic islet homeostasis and β-cell area in Stz mice possibly involves the attenuation of ER stress and inflammation (Engin et al., 2013). We believe that the islet and β-cell homeostasis improvement has contributed to the increase in insulin secretion observed in Stz mice treated with TUDCA.

Several landmark studies have revealed reduced brain insulin receptor sensitivity and insulin receptor (IR) expression in *post-mortem* AD brains (Chapman, Schiöth, Grillo, & Benedict, 2018). Insulin and its receptors are present in the brain, mainly in regions most vulnerable to AD neurodegeneration (de la Monte, 2017). In the brain, insulin regulates dendritic sprouting, neuronal stem cell activation, cell growth, synaptic plasticity and neuroprotection (Bedse et al., 2015), and also plays an important role in

learning and memory (Zhao, Chen, Quon, & Alkon, 2004). In this context, findings indicate that intranasal insulin administration improves AD symptomology (Chapman et al., 2018; De Felice, Lourenco, & Ferreira, 2014), enhancing cognition and Aβ clearance (de la Monte, 2017), and decreasing neuroinflammation (Rajasekar, Nath, Hanif, & Shukla, 2017). In our model, AD pathogenesis reduces IR β-subunit protein expression in the hippocampus, effect reversed by TUDCA treatment. The high levels of circulating insulin and the increase of insulin receptors in the hippocampus suggest that the action of insulin in this tissue must be potentiated by TUDCA.

Taken together, we concluded that TUDCA treatment improves glucose homeostasis in the streptozotocin-induced Alzheimer's disease mice model through distinguished mechanisms: improving glucose tolerance and peripheral insulin sensitivity, ameliorating insulin secretion, and increasing pancreatic β-cell area and islet mass. Both alterations contribute to the reduction in the pathological neuromarkers of AD in these mice. These findings suggest that TUDCA treatment is a potential strategy to counteract glucose homeostasis disturbance in AD pathology.

ACKNOWLEDGEMENTS

The authors thank Gabriela Rodrigues, Tatiane Ramos, and Wilson Floriano (Bil) for technical assistance.

CONFLICT OF INTEREST

The authors declared that they have no conflicts of interest.

FUNDING

This study was supported by the Fundação de Amparo à Pesquisa do Estado de São Paulo (FAPESP) (grant numbers: 2013/07607-8, 2015/12611-0, 2015/23729-1, 2017/13410-3, 2018/06363-1 and 2018/20213-2) and Conselho Nacional de Desenvolvimento Científico e Tecnológico (CNPq).

AUTHOR CONTRIBUTIONS

L.Z., J.F.V. and H.C.L.B.: designed the study; L.Z., J.F.V., C.S., G.A.B., D.F.E., M.A.K., G.M.S. and K.S.R.: conducted the experiments and acquired data; L.A.V., A.C.B., E.M.C. and H.C.L.B.: provided all reagents and supported the study; L.Z., J.F.V. and H.C.L.B. wrote and revised the manuscript. All authors reviewed and approved the final version of the manuscript.

REFERENCES

Abel, E. D., Peroni, O., Kim, J. K., Kim, Y. B., Boss, O., Hadro, E., . . . Kahn, B. B. (2001). Adipose-selective targeting of the GLUT4 gene impairs insulin action in muscle and liver. *Nature, 409*(6821), 729-733. doi:10.1038/35055575

Akinmokun, A., Selby, P. L., Ramaiya, K., & Alberti, K. G. (1992). The short insulin tolerance test for determination of insulin sensitivity: a comparison with the euglycaemic clamp. *Diabet Med, 9*(5), 432-437.

Antunes, M., & Biala, G. (2012). The novel object recognition memory: neurobiology, test procedure, and its modifications. *Cogn Process, 13*(2), 93-110. doi:10.1007/s10339-011-0430-z

Arvanitakis, Z., Bennett, D. A., Wilson, R. S., & Barnes, L. L. (2010). Diabetes and cognitive systems in older black and white persons. *Alzheimer Dis Assoc Disord, 24*(1), 37-42. doi:10.1097/WAD.0b013e3181a6bed5

Bedse, G., Di Domenico, F., Serviddio, G., & Cassano, T. (2015). Aberrant insulin signaling in Alzheimer's disease: current knowledge. *Front Neurosci, 9*, 204. doi:10.3389/fnins.2015.00204

Beeler, N., Riederer, B. M., Waeber, G., & Abderrahmani, A. (2009). Role of the JNK-interacting protein 1/islet brain 1 in cell degeneration in Alzheimer disease and diabetes. *Brain Res Bull, 80*(4-5), 274-281. doi:10.1016/j.brainresbull.2009.07.006

Biessels, G. J., Strachan, M. W., Visseren, F. L., Kappelle, L. J., & Whitmer, R. A. (2014). Dementia and cognitive decline in type 2 diabetes and prediabetic stages: towards targeted interventions. *Lancet Diabetes Endocrinol, 2*(3), 246-255. doi:10.1016/S2213-8587(13)70088-3

Boschero, A. C., Szpak-Glasman, M., Carneiro, E. M., Bordin, S., Paul, I., Rojas, E., & Atwater, I. (1995). Oxotremorine-m potentiation of glucose-induced insulin release from rat islets

involves M3 muscarinic receptors. *Am J Physiol, 268*(2 Pt 1), E336-342. doi:10.1152/ajpendo.1995.268.2.E336

Bruce, D. G., Casey, G. P., Grange, V., Clarnette, R. C., Almeida, O. P., Foster, J. K., . . . Study, F. C. i. D. (2003). Cognitive impairment, physical disability and depressive symptoms in older diabetic patients: the Fremantle Cognition in Diabetes Study. *Diabetes Res Clin Pract, 61*(1), 59-67. doi:10.1016/s0168-8227(03)00084-6

Cadavez, L., Montane, J., Alcarraz-Vizán, G., Visa, M., Vidal-Fàbrega, L., Servitja, J. M., & Novials, A. (2014). Chaperones ameliorate beta cell dysfunction associated with human islet amyloid polypeptide overexpression. *PLoS One, 9*(7), e101797. doi:10.1371/journal.pone.0101797

Chapman, C. D., Schiöth, H. B., Grillo, C. A., & Benedict, C. (2018). Intranasal insulin in Alzheimer's disease: Food for thought. *Neuropharmacology, 136*(Pt B), 196-201. doi:10.1016/j.neuropharm.2017.11.037

Clarke, J. R., Lyra E Silva, N. M., Figueiredo, C. P., Frozza, R. L., Ledo, J. H., Beckman, D., . . . De Felice, F. G. (2015). Alzheimer-associated Aβ oligomers impact the central nervous system to induce peripheral metabolic deregulation. *EMBO Mol Med, 7*(2), 190-210. doi:10.15252/emmm.201404183

Convit, A., Wolf, O. T., Tarshish, C., & de Leon, M. J. (2003). Reduced glucose tolerance is associated with poor memory performance and hippocampal atrophy among normal elderly. *Proc Natl Acad Sci U S A, 100*(4), 2019-2022. doi:10.1073/pnas.0336073100

Das, B., & Yan, R. (2017). Role of BACE1 in Alzheimer's synaptic function. *Transl Neurodegener, 6*, 23. doi:10.1186/s40035-017-0093-5

De Felice, F. G., Lourenco, M. V., & Ferreira, S. T. (2014). How does brain insulin resistance develop in Alzheimer's disease? *Alzheimers Dement, 10*(1 Suppl), S26-32. doi:10.1016/j.jalz.2013.12.004

de la Monte, S. M. (2017). Insulin Resistance and Neurodegeneration: Progress Towards the Development of New Therapeutics for Alzheimer's Disease. *Drugs, 77*(1), 47-65. doi:10.1007/s40265-016-0674-0

Decourt, B., Lahiri, D. K., & Sabbagh, M. N. (2017). Targeting Tumor Necrosis Factor Alpha for Alzheimer's Disease. *Curr Alzheimer Res, 14*(4), 412-425. doi:10.2174/1567205013666160930110551

Dionísio, P. A., Amaral, J. D., Ribeiro, M. F., Lo, A. C., D'Hooge, R., & Rodrigues, C. M. (2015). Amyloid-β pathology is attenuated by tauroursodeoxycholic acid treatment in APP/PS1 mice after disease onset. *Neurobiol Aging, 36*(1), 228-240. doi:10.1016/j.neurobiolaging.2014.08.034

Eleazu, C. O., Eleazu, K. C., Chukwuma, S., & Essien, U. N. (2013). Review of the mechanism of cell death resulting from streptozotocin challenge in experimental animals, its practical use and potential risk to humans. *J Diabetes Metab Disord, 12*(1), 60. doi:10.1186/2251-6581-12-60

Engin, F., Yermalovich, A., Nguyen, T., Ngyuen, T., Hummasti, S., Fu, W., . . . Hotamisligil, G. S. (2013). Restoration of the unfolded protein response in pancreatic β cells protects mice against type 1 diabetes. *Sci Transl Med, 5*(211), 211ra156. doi:10.1126/scitranslmed.3006534

Esser, N., Legrand-Poels, S., Piette, J., Scheen, A. J., & Paquot, N. (2014). Inflammation as a link between obesity, metabolic syndrome and type 2 diabetes. *Diabetes Res Clin Pract, 105*(2), 141-150. doi:10.1016/j.diabres.2014.04.006

Franco-Bocanegra, D. K., George, B., Lau, L. C., Holmes, C., Nicoll, J. A. R., & Boche, D. (2019). Microglial motility in Alzheimer's disease and after Aβ42 immunotherapy: a human post-mortem study. *Acta Neuropathol Commun, 7*(1), 174. doi:10.1186/s40478-019-0828-x

Furman, B. L. (2015). Streptozotocin-Induced Diabetic Models in Mice and Rats. *Curr Protoc Pharmacol, 70*, 5.47.41-20. doi:10.1002/0471141755.ph0547s70

Heneka, M. T., Carson, M. J., El Khoury, J., Landreth, G. E., Brosseron, F., Feinstein, D. L., . . . Kummer, M. P. (2015). Neuroinflammation in Alzheimer's disease. *Lancet Neurol, 14*(4), 388-405. doi:10.1016/S1474-4422(15)70016-5

Janson, J., Laedtke, T., Parisi, J. E., O'Brien, P., Petersen, R. C., & Butler, P. C. (2004). Increased risk of type 2 diabetes in Alzheimer disease. *Diabetes, 53*(2), 474-481. doi:10.2337/diabetes.53.2.474

Jiang, Z. Y., Zhou, Q. L., Coleman, K. A., Chouinard, M., Boese, Q., & Czech, M. P. (2003). Insulin signaling through Akt/protein kinase B analyzed by small interfering RNA-mediated gene silencing. *Proc Natl Acad Sci U S A, 100*(13), 7569-7574. doi:10.1073/pnas.1332633100

Kamat, P. K., Kalani, A., Rai, S., Tota, S. K., Kumar, A., & Ahmad, A. S. (2016). Streptozotocin Intracerebroventricular-Induced Neurotoxicity and Brain Insulin Resistance: a Therapeutic Intervention for Treatment of Sporadic Alzheimer's Disease (sAD)-Like Pathology. *Mol Neurobiol, 53*(7), 4548-4562. doi:10.1007/s12035-015-9384-y

Kang, S., Lee, Y. H., & Lee, J. E. (2017). Metabolism-Centric Overview of the Pathogenesis of Alzheimer's Disease. *Yonsei Med J, 58*(3), 479-488. doi:10.3349/ymj.2017.58.3.479

Keene, C. D., Rodrigues, C. M., Eich, T., Linehan-Stieers, C., Abt, A., Kren, B. T., . . . Low, W. C. (2001). A bile acid protects against motor and cognitive deficits and reduces striatal degeneration in the 3-nitropropionic acid model of Huntington's disease. *Exp Neurol, 171*(2), 351-360. doi:10.1006/exnr.2001.7755

Kinney, J. W., Bemiller, S. M., Murtishaw, A. S., Leisgang, A. M., Salazar, A. M., & Lamb, B. T. (2018). Inflammation as a central mechanism in Alzheimer's disease. *Alzheimers Dement (N Y), 4*, 575-590. doi:10.1016/j.trci.2018.06.014

Kurauti, M. A., Costa-Júnior, J. M., Ferreira, S. M., Dos Santos, G. J., Protzek, A. O., Nardelli, T. R., . . . Boschero, A. C. (2016). Acute exercise restores insulin clearance in diet-induced obese mice. *J Endocrinol, 229*(3), 221-232. doi:10.1530/JOE-15-0483

Lee, Y. Y., Hong, S. H., Lee, Y. J., Chung, S. S., Jung, H. S., Park, S. G., & Park, K. S. (2010). Tauroursodeoxycholate (TUDCA), chemical chaperone, enhances function of islets by reducing ER stress. *Biochem Biophys Res Commun, 397*(4), 735-739. doi:10.1016/j.bbrc.2010.06.022

Li, X., Song, D., & Leng, S. X. (2015). Link between type 2 diabetes and Alzheimer's disease: from epidemiology to mechanism and treatment. *Clin Interv Aging, 10*, 549-560. doi:10.2147/CIA.S74042

Lo, A. C., Callaerts-Vegh, Z., Nunes, A. F., Rodrigues, C. M., & D'Hooge, R. (2013). Tauroursodeoxycholic acid (TUDCA) supplementation prevents cognitive impairment and amyloid deposition in APP/PS1 mice. *Neurobiol Dis, 50*, 21-29. doi:10.1016/j.nbd.2012.09.003

Lowell, B. B., & Shulman, G. I. (2005). Mitochondrial dysfunction and type 2 diabetes. *Science, 307*(5708), 384-387. doi:10.1126/science.1104343

Macklin, L., Griffith, C. M., Cai, Y., Rose, G. M., Yan, X. X., & Patrylo, P. R. (2017). Glucose tolerance and insulin sensitivity are impaired in APP/PS1 transgenic mice prior to amyloid plaque pathogenesis and cognitive decline. *Exp Gerontol, 88*, 9-18. doi:10.1016/j.exger.2016.12.019

Mittal, K., & Katare, D. P. (2016). Shared links between type 2 diabetes mellitus and Alzheimer's disease: A review. *Diabetes Metab Syndr, 10*(2 Suppl 1), S144-149. doi:10.1016/j.dsx.2016.01.021

Müller, D., Nitsch, R. M., Wurtman, R. J., & Hoyer, S. (1998). Streptozotocin increases free fatty acids and decreases phospholipids in rat brain. *J Neural Transm (Vienna), 105*(10-12), 1271-1281. doi:10.1007/s007020050130

Nath, S., Ghosh, S. K., & Choudhury, Y. (2017). A murine model of type 2 diabetes mellitus developed using a combination of high fat diet and multiple low doses of streptozotocin treatment mimics the metabolic characteristics of type 2 diabetes mellitus in humans. *J Pharmacol Toxicol Methods, 84*, 20-30. doi:10.1016/j.vascn.2016.10.007

Nunes, A. F., Amaral, J. D., Lo, A. C., Fonseca, M. B., Viana, R. J., Callaerts-Vegh, Z., . . . Rodrigues, C. M. (2012). TUDCA, a bile acid, attenuates amyloid precursor protein processing and amyloid-β deposition in APP/PS1 mice. *Mol Neurobiol, 45*(3), 440-454. doi:10.1007/s12035-012-8256-y

Ozcan, U., Yilmaz, E., Ozcan, L., Furuhashi, M., Vaillancourt, E., Smith, R. O., . . . Hotamisligil, G. S. (2006). Chemical chaperones reduce ER stress and restore glucose homeostasis in a mouse model of type 2 diabetes. *Science, 313*(5790), 1137-1140. doi:10.1126/science.1128294

Pająk, B., Kania, E., & Orzechowski, A. (2016). Killing Me Softly: Connotations to Unfolded Protein Response and Oxidative Stress in Alzheimer's Disease. *Oxid Med Cell Longev, 2016*, 1805304. doi:10.1155/2016/1805304

Pekny, M., & Nilsson, M. (2005). Astrocyte activation and reactive gliosis. *Glia, 50*(4), 427-434. doi:10.1002/glia.20207

Peron, R., Vatanabe, I. P., Manzine, P. R., Camins, A., & Cominetti, M. R. (2018). Alpha-Secretase ADAM10 Regulation: Insights into Alzheimer's Disease Treatment. *Pharmaceuticals (Basel), 11*(1). doi:10.3390/ph11010012

Plaschke, K., & Hoyer, S. (1993). Action of the diabetogenic drug streptozotocin on glycolytic and glycogenolytic metabolism in adult rat brain cortex and hippocampus. *Int J Dev Neurosci, 11*(4), 477-483. doi:10.1016/0736-5748(93)90021-5

Rai, S., Kamat, P. K., Nath, C., & Shukla, R. (2014). Glial activation and post-synaptic neurotoxicity: the key events in Streptozotocin (ICV) induced memory impairment in rats. *Pharmacol Biochem Behav, 117*, 104-117. doi:10.1016/j.pbb.2013.11.035

Rajasekar, N., Nath, C., Hanif, K., & Shukla, R. (2017). Intranasal Insulin Administration Ameliorates Streptozotocin (ICV)-Induced Insulin Receptor Dysfunction, Neuroinflammation, Amyloidogenesis, and Memory Impairment in Rats. *Mol Neurobiol, 54*(8), 6507-6522. doi:10.1007/s12035-016-0169-8

Ravelli, K. G., Rosário, B. D., Camarini, R., Hernandes, M. S., & Britto, L. R. (2017). Intracerebroventricular Streptozotocin as a Model of Alzheimer's Disease: Neurochemical and Behavioral Characterization in Mice. *Neurotox Res, 31*(3), 327-333. doi:10.1007/s12640-016-9684-7

Rudrabhatla, P., Jaffe, H., & Pant, H. C. (2011). Direct evidence of phosphorylated neuronal intermediate filament proteins in neurofibrillary tangles (NFTs): phosphoproteomics of Alzheimer's NFTs. *FASEB J, 25*(11), 3896-3905. doi:10.1096/fj.11-181297

Salkovic-Petrisic, M., & Hoyer, S. (2007). Central insulin resistance as a trigger for sporadic Alzheimer-like pathology: an experimental approach. *J Neural Transm Suppl*(72), 217-233. doi:10.1007/978-3-211-73574-9_28

Salkovic-Petrisic, M., Osmanovic, J., Grünblatt, E., Riederer, P., & Hoyer, S. (2009). Modeling sporadic Alzheimer's disease: the insulin resistant brain state generates multiple long-term morphobiological abnormalities including hyperphosphorylated tau protein and amyloid-beta. *J Alzheimers Dis, 18*(4), 729-750. doi:10.3233/JAD-2009-1184

Selkoe, D. J. (2001). Alzheimer's disease: genes, proteins, and therapy. *Physiol Rev, 81*(2), 741-766. doi:10.1152/physrev.2001.81.2.741

Shinohara, M., & Sato, N. (2017). Bidirectional interactions between diabetes and Alzheimer's disease. *Neurochem Int, 108*, 296-302. doi:10.1016/j.neuint.2017.04.020

Thambisetty, M., Jeffrey Metter, E., Yang, A., Dolan, H., Marano, C., Zonderman, A. B., . . . O'Brien, R. J. (2013). Glucose intolerance, insulin resistance, and pathological features

of Alzheimer disease in the Baltimore Longitudinal Study of Aging. *JAMA Neurol, 70*(9), 1167-1172. doi:10.1001/jamaneurol.2013.284

Vandal, M., White, P. J., Chevrier, G., Tremblay, C., St-Amour, I., Planel, E., . . . Calon, F. (2015). Age-dependent impairment of glucose tolerance in the 3xTg-AD mouse model of Alzheimer's disease. *FASEB J, 29*(10), 4273-4284. doi:10.1096/fj.14-268482

Vandal, M., White, P. J., Tremblay, C., St-Amour, I., Chevrier, G., Emond, V., . . . Calon, F. (2014). Insulin reverses the high-fat diet-induced increase in brain Aβ and improves memory in an animal model of Alzheimer disease. *Diabetes, 63*(12), 4291-4301. doi:10.2337/db14-0375

Vanhanen, M., Koivisto, K., Kuusisto, J., Mykkänen, L., Helkala, E. L., Hänninen, T., . . . Laakso, M. (1998). Cognitive function in an elderly population with persistent impaired glucose tolerance. *Diabetes Care, 21*(3), 398-402. doi:10.2337/diacare.21.3.398

Vettorazzi, J. F., Kurauti, M. A., Soares, G. M., Borck, P. C., Ferreira, S. M., Branco, R. C. S., . . . Carneiro, E. M. (2017). Bile acid TUDCA improves insulin clearance by increasing the expression of insulin-degrading enzyme in the liver of obese mice. *Sci Rep, 7*(1), 14876. doi:10.1038/s41598-017-13974-0

Vettorazzi, J. F., Ribeiro, R. A., Borck, P. C., Branco, R. C., Soriano, S., Merino, B., . . . Carneiro, E. M. (2016). The bile acid TUDCA increases glucose-induced insulin secretion via the cAMP/PKA pathway in pancreatic beta cells. *Metabolism, 65*(3), 54-63. doi:10.1016/j.metabol.2015.10.021

Walsh, D. M., & Selkoe, D. J. (2004). Deciphering the molecular basis of memory failure in Alzheimer's disease. *Neuron, 44*(1), 181-193. doi:10.1016/j.neuron.2004.09.010

Wang, J., Gu, B. J., Masters, C. L., & Wang, Y. J. (2017). A systemic view of Alzheimer disease - insights from amyloid-β metabolism beyond the brain. *Nat Rev Neurol, 13*(10), 612-623. doi:10.1038/nrneurol.2017.111

Yin, F., Sancheti, H., Patil, I., & Cadenas, E. (2016). Energy metabolism and inflammation in brain aging and Alzheimer's disease. *Free Radic Biol Med, 100*, 108-122. doi:10.1016/j.freeradbiomed.2016.04.200

Zangerolamo, L., Soares, G. M., Vettorazzi, J. F., do Amaral, M. E., Carneiro, E. M., Olalla-Saad, S. T., . . . Barbosa-Sampaio, H. C. (2019). ARHGAP21 deficiency impairs hepatic lipid metabolism and improves insulin signaling in lean and obese mice. *Can J Physiol Pharmacol, 97*(11), 1018-1027. doi:10.1139/cjpp-2018-0691

Zhang, Y. W., Thompson, R., Zhang, H., & Xu, H. (2011). APP processing in Alzheimer's disease. *Mol Brain, 4*, 3. doi:10.1186/1756-6606-4-3

Zhao, W. Q., Chen, H., Quon, M. J., & Alkon, D. L. (2004). Insulin and the insulin receptor in experimental models of learning and memory. *Eur J Pharmacol, 490*(1-3), 71-81. doi:10.1016/j.ejphar.2004.02.045

Zisman, A., Peroni, O. D., Abel, E. D., Michael, M. D., Mauvais-Jarvis, F., Lowell, B. B., . . . Kahn, B. B. (2000). Targeted disruption of the glucose transporter 4 selectively in muscle causes insulin resistance and glucose intolerance. *Nat Med, 6*(8), 924-928. doi:10.1038/78693

FIGURE LEGENDS

Figure 1. TUDCA attenuates the AD biomarkers in Stz mice. Brain weight (A). Protein content of Amyloid Oligomer (B) normalized by GAPDH in hippocampus. Representative images of microglia in the hippocampus. Iba-1 immunoreactivity (green), scale bars 100 μm (C) and quantification of Iba-1 positive staining in the hippocampus (D). Preference index in NORT (E). Hippocampal gene expression of TNF-α, IL-1β, IL-6, IFN-γ, GFAP, APP, ADAM-10, X11-α, BACE-1 and BDNF (F) normalized by GAPDH. Protein content of IR β-subunit (G) normalized by GAPDH in hippocampus. Data are the mean ± SEM (n=5-7). Different letters indicate significant differences between groups and * indicates no significant difference compared to the fixed value of 50% ($P \leq 0.05$). Statistical analysis was performed by one-way ANOVA followed by Tukey post-hoc-test. CA: *cornus ammon*, DG: dentate gyrus, AU: arbitrary units.

Figure 2. TUDCA treatment improves glucose tolerance, insulin sensitivity and fasting and fed glycemia in Stz mice. Changes in blood glucose (A) and AUC of blood glucose (B) during ipGTT. Changes in blood glucose (C) and rate constant for glucose disappearance (kITT) (D) during the ipITT. Fasting (E) and Fed (F) glycemia. Data are the mean ± SEM (n=5-7). Different letters indicate significant differences between groups and * indicates Stz is different from Ctl and Stz+TUDCA mice ($P \leq 0.05$). Statistical analysis was performed by one-way ANOVA followed by Tukey post-hoc-test.

Figure 3. TUDCA treatment increases glucose-stimulated insulin secretion and does not modulate insulin clearance in Stz mice. Plasmatic c-peptide (A) and insulin (B) and c-peptide:insulin ratio (C) before and 30 and 60 min after a glucose gavage and

AUC of plasma c-peptide:insulin ratio (D). Protein content of IDE (E) and CEACAM-1 (F) normalized by GAPDH in the liver. Insulin secretion of isolated pancreatic islets after 1 hr incubation with 2.8 and 11.1 mM glucose (G) and total insulin content of islets (H). Data are the mean ± SEM (n=5-7). Different letters indicate significant differences between groups ($P \leq 0.05$). Statistical analysis was performed by one-way ANOVA followed by Tukey post-hoc-test. AU: arbitrary units.

Figure 4. TUDCA treatment increases β-cell number per islet and total β-cell in Stz mice. Pancreas weight (mg) (A). Total islet area (μm^2) (B). Islet/Pancreas section ratio (C). Islets mass (mg) (D). β-cell mass (mg) (E). β-cell/islet ratio (F). Total β-cell (μm^2) (G). Representative images of pancreas sections stained for insulin (H). Data are the mean ± SEM (n=5). Different letters indicate significant differences between groups ($P \leq 0.05$). Statistical analysis was performed by one-way ANOVA followed by Tukey post-hoc-test.

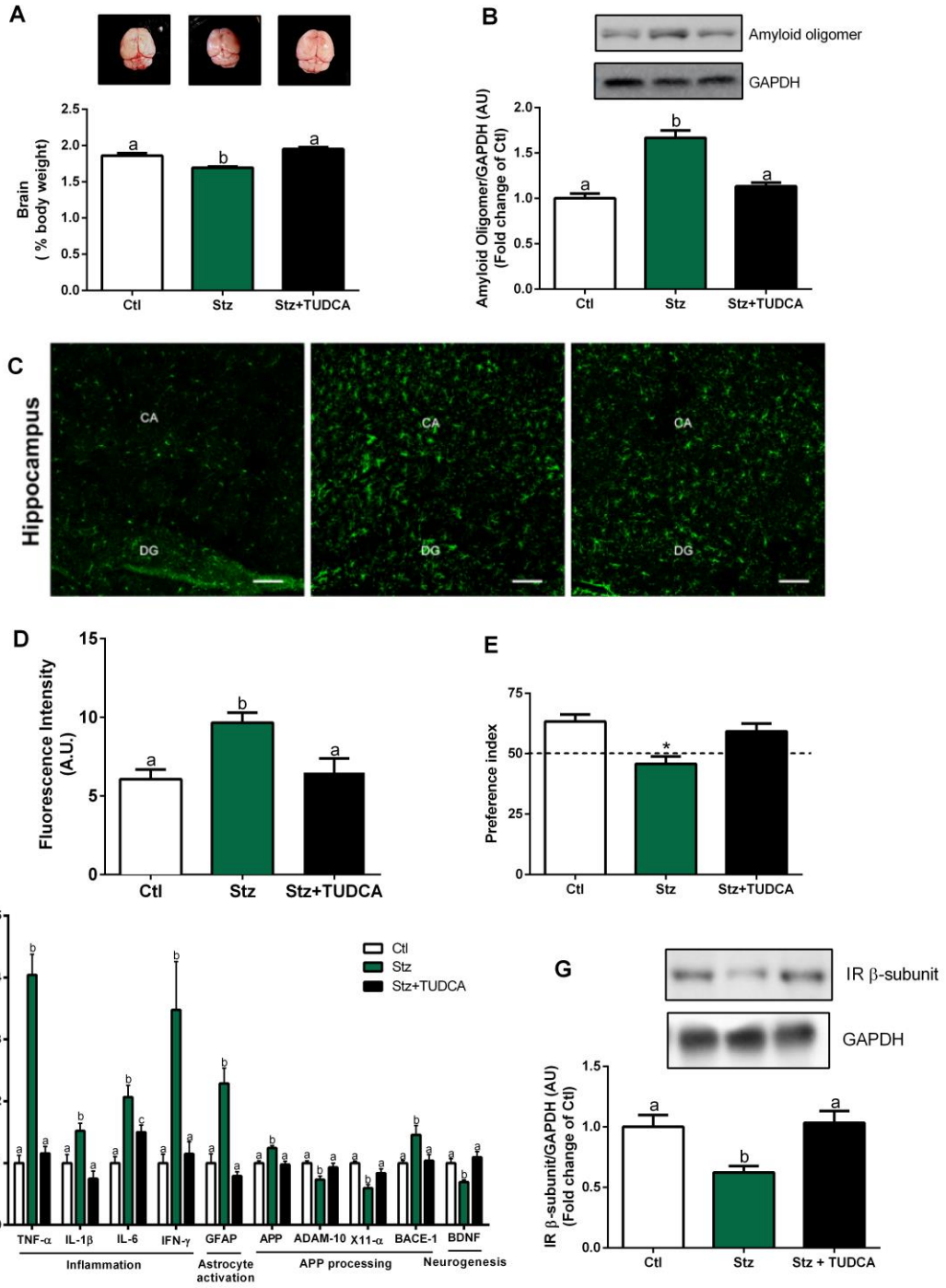
A
Brain
(% body weight)
Ctl
Stz
Stz+TUDCA
B
Amyloid oligomer
GAPDH
Amyloid Oligomer/GAPDH (AU)
(Fold change of Ctl)
C
Hippocampus
CA
DG
D
Fluorescence Intensity
(A.U.)
E
Preference index
F
Gene expression/GAPDH mRNA
(Fold change of Ctl)
TNF-α
IL-1β
IL-6
IFN-γ
GFAP
APP
ADAM-10
X11-α
BACE-1
BDNF
Inflammation
Astrocyte activation
APP processing
Neurogenesis
G
IR β-subunit
GAPDH
IR β-subunit/GAPDH (AU)
(Fold change of Ctl)
Stz + TUDCA

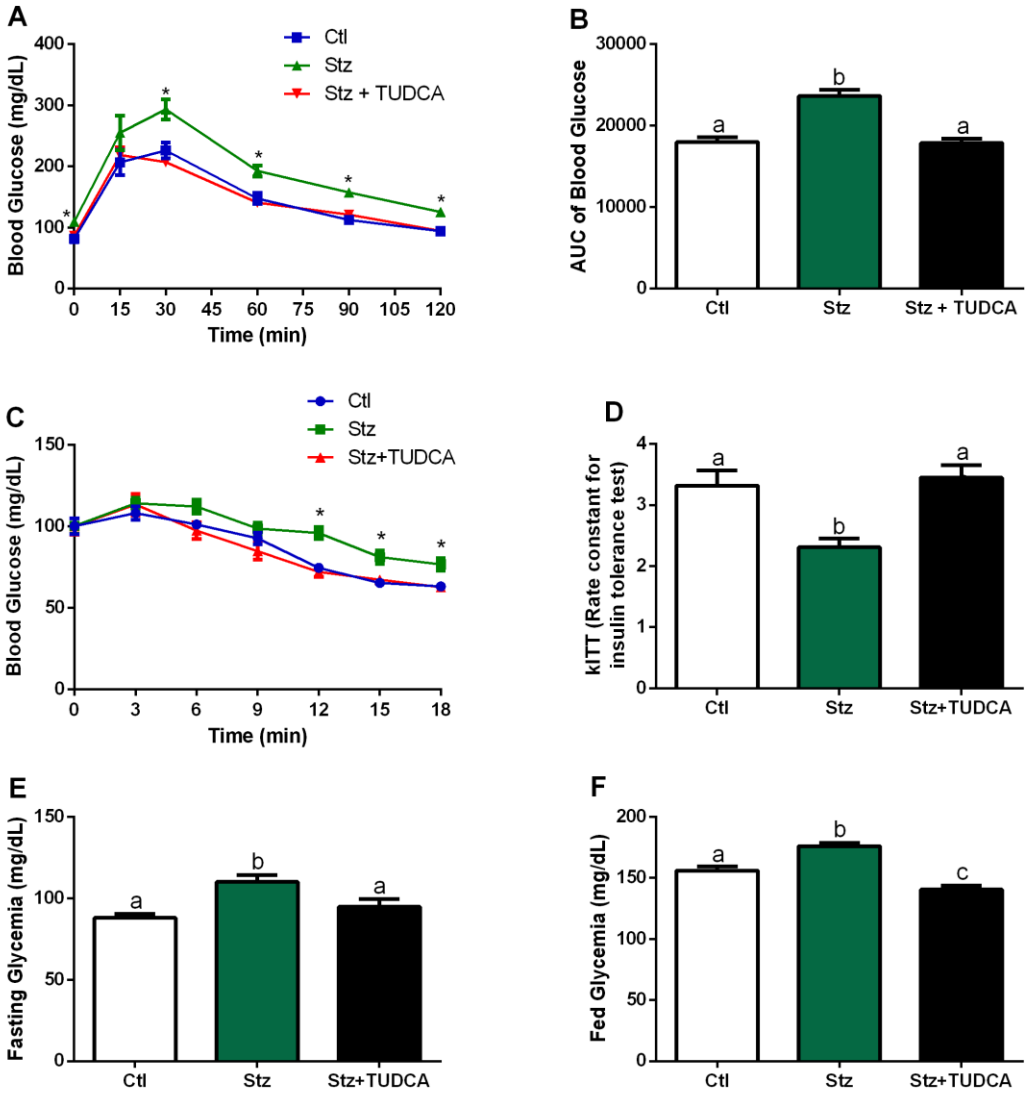
A
Blood Glucose (mg/dL)
Time (min)
Ctl
Stz
Stz + TUDCA
B
AUC of Blood Glucose
C
Blood Glucose (mg/dL)
Time (min)
Ctl
Stz
Stz+TUDCA
D
kITT (Rate constant for insulin tolerance test)
E
Fasting Glycemia (mg/dL)
F
Fed Glycemia (mg/dL)

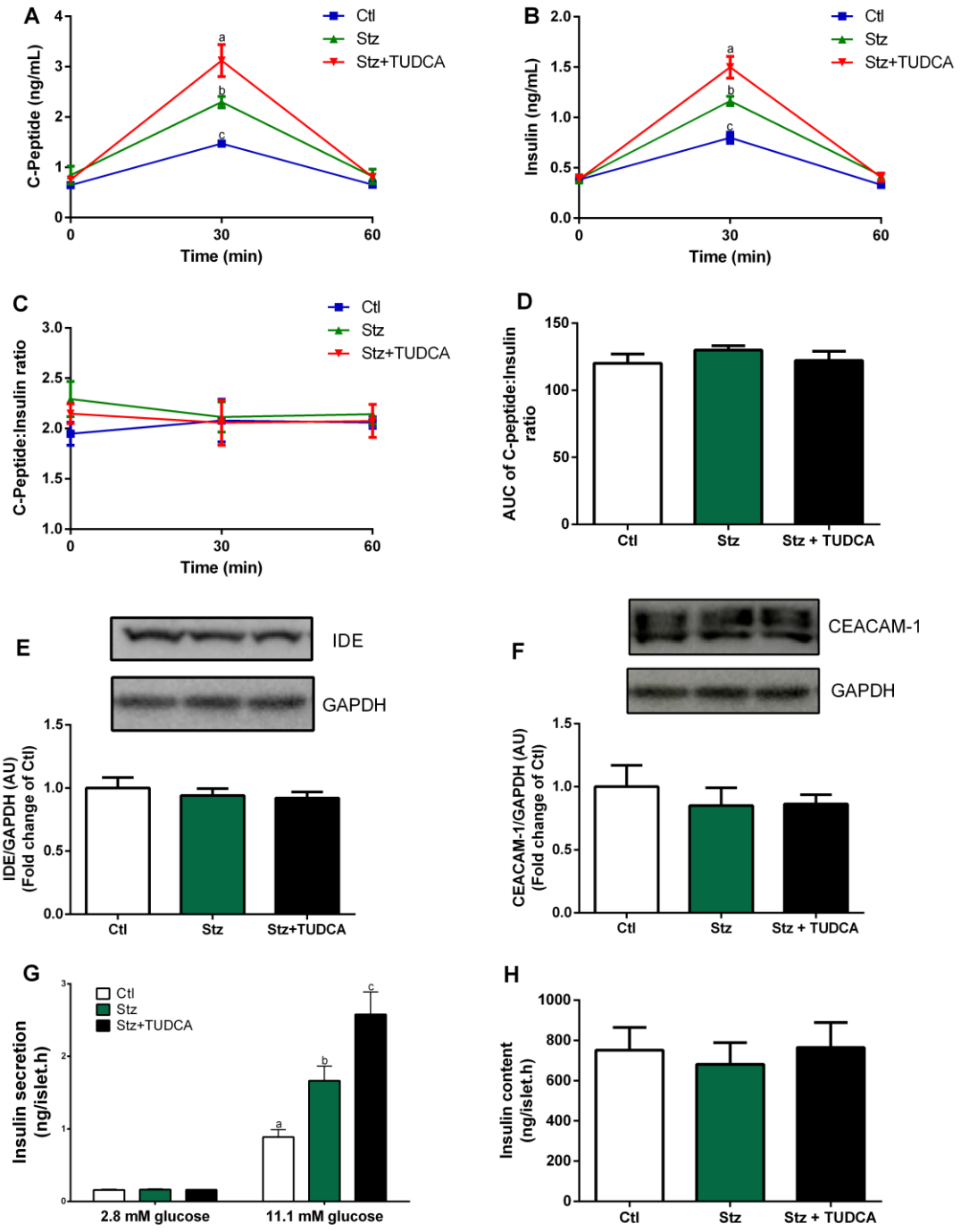
A
C-Peptide (ng/mL)
Time (min)
Ctl
Stz
Stz+TUDCA
B
Insulin (ng/mL)
C
C-Peptide:Insulin ratio
D
AUC of C-peptide:Insulin ratio
Ctl
Stz
Stz + TUDCA
E
IDE
GAPDH
IDE/GAPDH (AU) (Fold change of Ctl)
F
CEACAM-1
GAPDH
CEACAM-1/GAPDH (AU) (Fold change of Ctl)
G
Insulin secretion (ng/islet.h)
2.8 mM glucose
11.1 mM glucose
H
Insulin content (ng/islet.h)

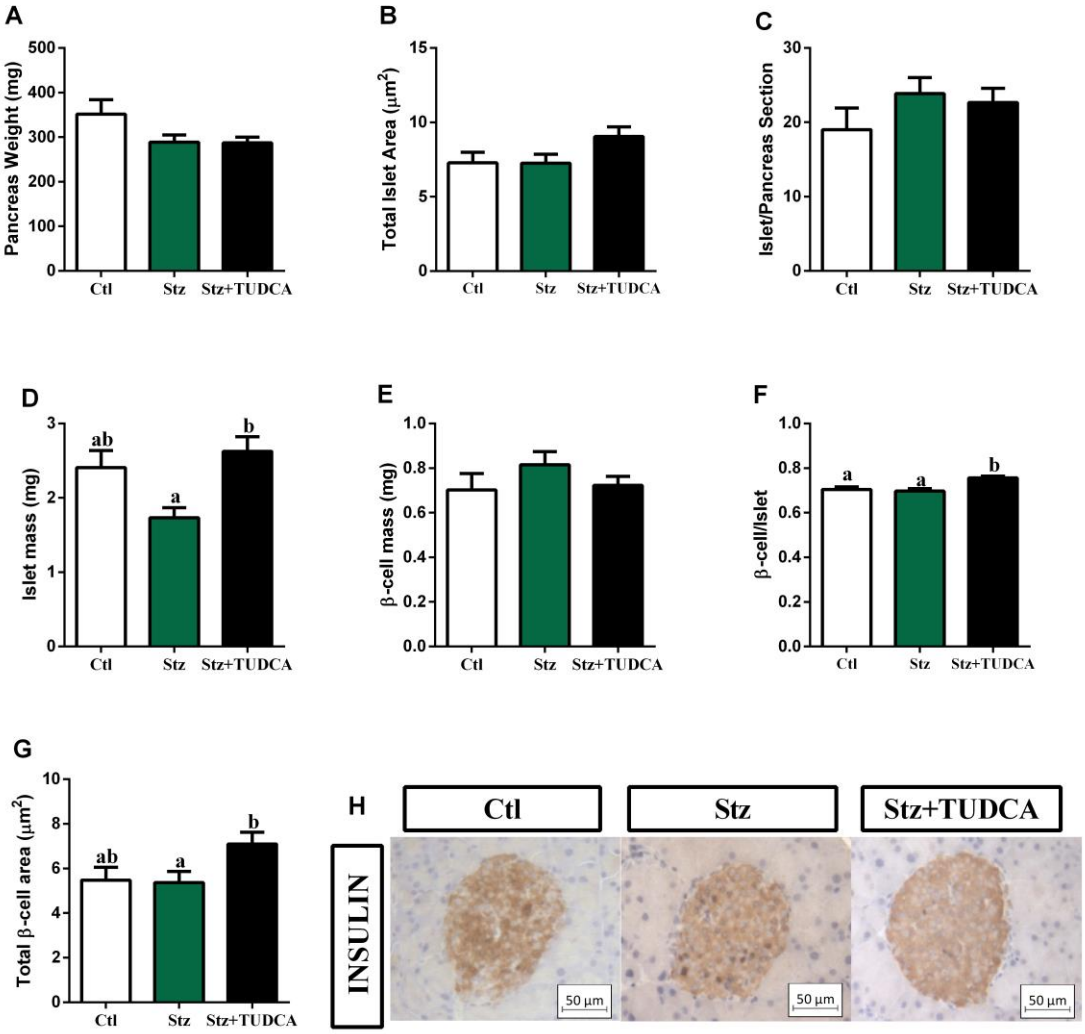
A
Pancreas Weight (mg)
500
400
300
200
100
0
Ctl
Stz
Stz+TUDCA
B
Total Islet Area (μm²)
15
10
5
0
Ctl
Stz
Stz+TUDCA
C
Islet/Pancreas Section
30
20
10
0
Ctl
Stz
Stz+TUDCA
D
Islet mass (mg)
3
2
1
0
ab
a
b
Ctl
Stz
Stz+TUDCA
E
β-cell mass (mg)
1.0
0.8
0.6
0.4
0.2
0.0
Ctl
Stz
Stz+TUDCA
F
β-cell/Islet
1.0
0.8
0.6
0.4
0.2
0.0
a
a
b
Ctl
Stz
Stz+TUDCA
G
Total β-cell area (μm²)
10
8
6
4
2
0
ab
a
b
Ctl
Stz
Stz+TUDCA
H
Ctl
Stz
Stz+TUDCA
INSULIN
50 μm
50 μm
50 μm

Table 1: Primer sequences for real-time qPCR assays.

Gene	Forward (5' – 3')	Reverse (3' – 5')
TNF-α	CCCTCACACTCAGATCATCTTCT	GCTACGACGTGGGCTACAG
IL-1β	GCAACTGTTCCTGAACTCAACT	ATCTTTTGGGGTCCGTCAACT
IL-6	TAGTCCTTCCTACCCCAATTTCC	TTGGTCCTTAGCCACTCCTTC
IFN-$_{\gamma}$	ATGAACGCTACACACTGCATC	CCATCCTTTTGCCAGTTCCTC
GFAP	CCCTGGCTCGTGTGGATTT	GACCGATACCACTCCTCTGTC
BDNF	TCATACTTCGGTTGCATGAAGG	AGACCTCTCGAACCTGCCC
ADAM-10	ATGGTGTTGCCGACAGTGTTA	GTTTGGCACGCTGGTGTTTTT
BACE-1	GGAACCCATCTCGGCATCC	TCCGATTCCTCGTCGGTCTC
X11-α	GGTGCTGAGTCATCAAGCATAC	GAACTTCAACGTAGGTTGGGAA
GAPDH	AGGTCGGTGTGAACGGATTTG	AGTAGACCATGTAGTTGAGGTCA

TNF-α: tumor necrosis factor alpha; IL-1β: interleukin 1 beta; IL-6: interleukin 6; IFN-$_{\gamma}$: interferon gamma; GFAP: glial fibrillary acidic protein; BDNF: brain-derived neurotrophic factor; ADAM-10: a disintegrin and metalloproteinase 10; BACE-1: beta-secretase 1; X11-α: X11 alpha; GAPDH: glyceraldehyde 3-phosphate dehydrogenase.

Table 2: Final characterization of Ctl, Stz and Stz+TUDCA mice

	Ctl	Stz	Stz+TUDCA
Body weight (BW) (g)	24.39 ± 0.21[a]	25.72 ± 0.38[b]	23.47 ± 0.48[a]
Skeletal muscle pad (% BW)	1.034 ± 0.033	1.019 ± 0.041	0.949 ± 0.028
Perigonadal fat pad (% BW)	0.390 ± 0.040[a]	0.625 ± 0.090[b]	0.333 ± 0.037[a]
Retroperitoneal fat pad (% BW)	0.064 ± 0.004[a]	0.096 ± 0.011[b]	0.067 ± 0.005[a]

Different letters indicate significant difference (one-way ANOVA followed by Tukey post-hoc-test, $P \leq 0.05$). Data are the mean ± SEM (n = 6–9).

Supplementary Figure

The bile acid TUDCA improves glucose metabolism in streptozotocin-induced Alzheimer's disease mice model

Lucas Zangerolamo[1], Jean F. Vettorazzi[2], Carina Solon[3], Gabriela A. Bronczek[1], Daiane F. Engel[3], Mirian A. Kurauti[4], Gabriela M. Soares[1], Karina S. Rodrigues[1], Lício A. Velloso[3], Antonio C. Boschero[1], Everardo M. Carneiro[1], Helena C. L. Barbosa[1*]

[1] Obesity and Comorbidities Research Center, Department of Structural and Functional Biology, University of Campinas, UNICAMP, Campinas, Sao Paulo, Brazil.

[2] Educational Union of Cascavel, UNIVEL, Cascavel, Parana, Brazil.

[3] Laboratory of Cell Signaling, Obesity and Comorbidities Research Center, University of Campinas, UNICAMP, Campinas, Sao Paulo, Brazil.

[4] Department of Physiological Sciences, State University of Maringa, UEM, Maringa, Parana, Brazil.

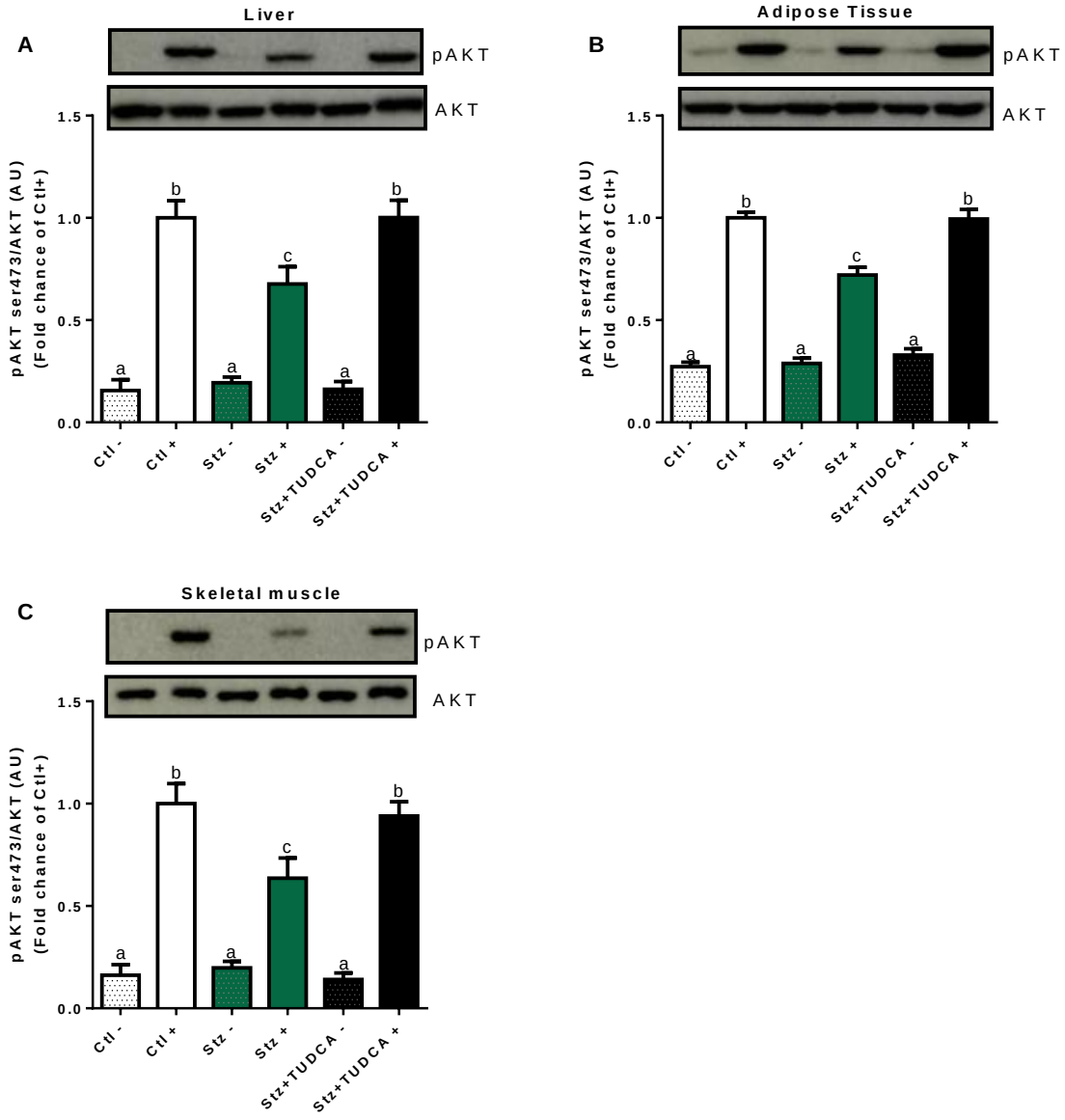

Supplementary Figure 1: TUDCA treatment increases AKT phosphorylation levels in peripheral tissues of Stz mice. Protein content of pAKT (Ser473) normalized by total AKT in liver (A), adipose tissue (B) and skeletal muscle (C) before (-) and 5 min after (+) 4U/kg insulin load. Data are the mean ± SEM (n=5-7). Different letters indicate significant differences between groups ($P \leq 0.05$). Statistical analysis was performed by one-way ANOVA followed by Tukey post-hoc-test. AU: arbitrary units.